

**ANALYSIS AND AN IMAGE RECOVERY ALGORITHM
FOR ULTRASONIC TOMOGRAPHY SYSTEM**

Michael Y. Jin
Jet Propulsion Laboratory
California Institute of Technology
Pasadena, California 91109

ABSTRACT

The problem of an ultrasonic reflectivity tomography is similar to that of a spotlight-mode aircraft Synthetic Aperture Radar (SAR) system. The analysis for a circular path spotlight mode SAR in this paper leads to the insight of the system characteristics. It indicates that such a system when operated in a wide bandwidth is capable of achieving the ultimate resolution; one quarter of the wavelength of the carrier frequency. An efficient processing algorithm based on the exact two dimensional spectrum is presented. The results of simulation indicate that the impulse responses meet the predicted resolution performance. Compared to an algorithm previously developed for the ultrasonic reflectivity tomography, the throughput rate of this algorithm is about ten times higher.

INTRODUCTION

The geometry of a two dimensional reflectivity tomography can be depicted in Figure 1.a. It consists of a water tank of dimensions greater than that of the object to be imaged. A moving transducer and a receiver are scanning over the outer circle. Ultrasonic pulses are emitted from the transducer. Signals reflected from the object are sensed by the receiver and collected for further processing. For simplification, we shall consider that the transducer and receiver are collocated. Furthermore, the object shall be an idealized reflecting medium in which the velocity of the sound is constant, the medium is weakly reflecting, and absorption is uniform over the region of interest [1].

A spotlight mode SAR in circular path as shown in Figure 1.b is analogous to the reflectivity tomography system addressed here. In this SAR system, the altitude is assumed to be much smaller than the radius of the flight circle. The pulses transmitted periodically from the radar is a wide band electro-magnetic wave traveling at a constant speed in the atmosphere. The signal reflected from the ground spot within the radar footprint is received by the same radar used for emitting radar pulses. Echo signals are demodulated by the carrier frequency, converted into discrete digital format, and stored in an on-board recorder. The stored data will be processed by an on-board or ground based processor to reveal the ground image. The design of the radar pulse and echo timing for both systems must be coherent.

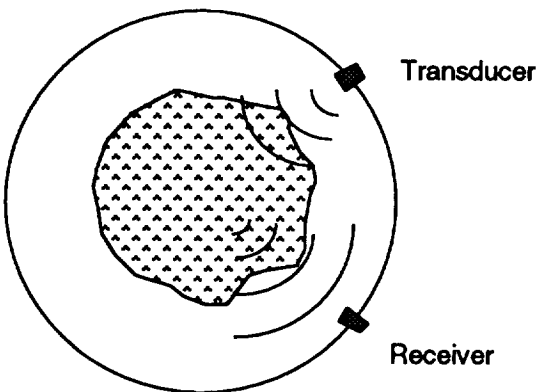


Figure 1.a The reflectivity tomography system

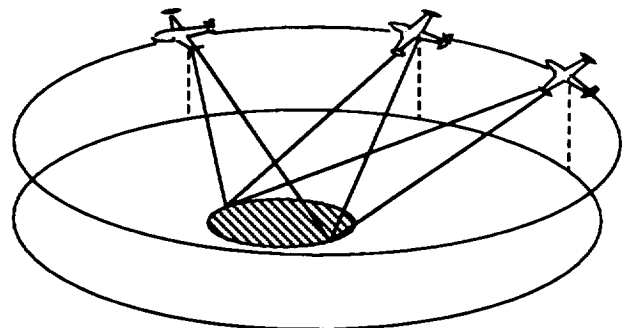


Figure 1.b A circular path spotlight mode SAR

Since the analysis and processing algorithm description for such systems were originated from the spotlight-mode SAR system, it will also be given in the following paragraph. However, it should be noted that both the analysis and processing algorithm are applicable to the ultrasonic reflectivity system as shown in Figure 1.a.

ANALYSIS

A wide azimuth beam SAR can offer higher resolution or wider azimuth viewing angle; two factors that help better characterize the backscattering property of targets for various scientific applications. One disadvantage of a wide beam SAR is that a much higher pulse repetition frequency (PRF) is usually required since PRF is proportional to the radar beam angle. This problem can be resolved using a spotlight-mode concept: steering a narrow beam SAR to a fixed spot on the ground. The drawback of a spotlight-mode SAR is its limited coverage.

A spotlight-mode SAR can be operated from a circular flight path as shown in Figure 1.b. This type of spotlight-mode SAR offers several advantages: (1) relatively easy to achieve the ultimate azimuth resolution, (2) it allows a full 360 degree of viewing angle, (3) there is no need to steer the radar, and (4) the required PRF can be scaled down according to the ratio between the radius of the radar spot to the radius of the flight path.

For an aircraft SAR in a circular path as shown in Figure 2, the slant range history of a point-target is given by

$$R(\theta_1) = \sqrt{A + B \cdot \cos \theta_1}$$

where

$$A = R_0^2 + 2R_b^2 - 2R_0R_b \cos \theta_e, \text{ and } B = 2R_b(R_0 \cos \theta_e - R_b).$$

In the above equations, θ_e is the radar elevation angle, R_0 is slant range between the radar and the target at the beam center, R_b is the radius of the flight path, and θ_1 is the angle between the radar at the minimum range to the target, the center of the flight circle, and the radar at time of interest. Since time is directly proportional to θ_1 , this function can also be expressed using time as the variable,

$$R(t) = \sqrt{A + B \cdot \cos\left(\frac{v}{R_b}t\right)}$$

where v is the speed of the aircraft. Let Z denotes the altitude of the aircraft. It is obvious that R_0 and Z are related by $Z = R_0 \sin \theta_e$. $Z=0$ is a special case that exactly follows the geometry of the ultrasonic reflectivity tomography as shown in Figure 1.a. Below, we shall denote the distance between the target and the center of the path projection on the ground as R_T , which is equal to $R_b - R_0 \cos \theta_e$.

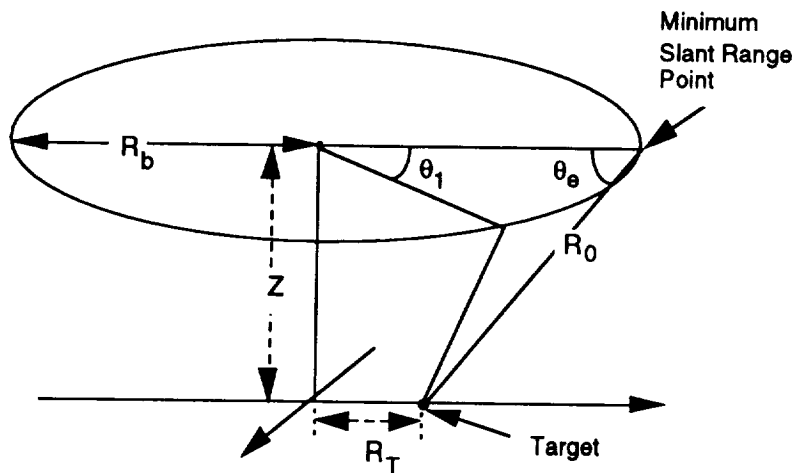


Figure 2. The spotlight SAR platform geometry

To provide better insight into the spot-light SAR characteristics, it is assumed that the radar beam width is unlimited such that any target within the path projection is illuminated all the time during mapping. To determine the azimuth resolution, it is necessary to determine the maximum Doppler bandwidth. This can be accomplished by evaluating the zero crossing time of the Doppler frequency rate. The Doppler history is the derivative of the slant range, i.e.

$$f_d(t) = \frac{-d(2R(t)/\lambda)}{dt} = \frac{k_0 Bv}{2\pi R_b} \sin\left(\frac{vt}{R_b}\right) R^{-1}(t)$$

where k_0 is the wave number and is equal to $2\pi/\lambda$. λ is the wave length corresponding to the center frequency of the radar pulse. Plots of both the slant range history and Doppler history are given in Figure 3a and b. The history of the Doppler frequency begins with 0Hz at the minimum slant range point, decreases to the minimum Doppler (negative value), increases back to 0Hz at the maximum slant range point, keeps increasing up to the maximum Doppler, and then decreases back to 0Hz after a complete cycle. Based on this, one can divide a complete circle into two apertures with equivalent bandwidth. The aperture with a Doppler ranging from its minimum to its maximum and consisting of the minimum slant range point is referred to as the **principle aperture**. The other aperture spanning the rest of the flight path is referred to as the **complement aperture**.

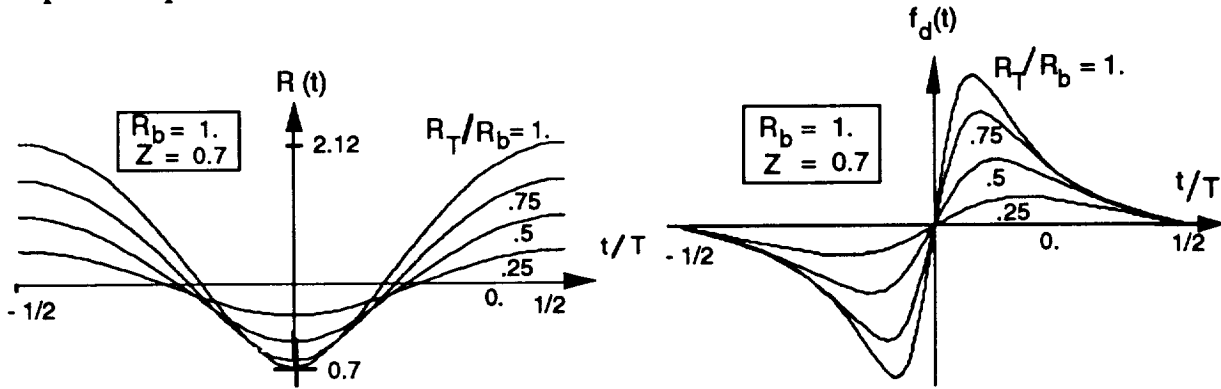


Figure 3.a Slant range history plots

Figure 3.b Doppler frequency history plots

The Doppler frequency rate variation is given by

$$f_r(t) = \frac{df_d}{dt} = \frac{k_0 Bv}{2\pi R_b} \left(\frac{v}{R_b} \cos\left(\frac{vt}{R_b}\right) R^{-1}(t) + \frac{Bv}{2R_b} \sin^2\left(\frac{vt}{R_b}\right) R^{-3}(t) \right)$$

The solution of the time at which f_r equals zero is given by

$$t|_{f_r=0} = \frac{R_b}{v} \cos^{-1} \left(\frac{-A \pm (A^2 - B^2)^{1/2}}{B} \right)$$

Therefore, the Doppler bandwidth, denoted as F , is given by two times the absolute value of the Doppler at one of the solution given above. Since F varies as a function of both the aircraft altitude Z and target radius R_T , it is given by

$$F(Z, R_T) = \frac{2\sqrt{2v}}{\lambda R_b} (A^2 - B^2)^{-1/4} \sqrt{|A^2 - B^2 - A\sqrt{A^2 - B^2}|}$$

The azimuth resolution is thus given by the reciprocal of the bandwidth multiplied with the effective velocity $(R_T/R_b)v$, or

$$\Delta X(Z, R_T) = \left(\frac{R_T}{R_b} v \right) \frac{1}{F(Z, R_T)}$$

The variations of the resolution and the Doppler bandwidth as a function of the target location are plotted in Figure 4.a and Figure 4.b. It should be noted that these plots also include the targets located outside of the vertical cylinder containing the orbit because they can also be imaged as long as range ambiguity can be avoided. It is interesting to see that the ultimate resolution of $\lambda/4$ can be achieved for targets falling on the orbit plane and bounded by the circular orbit. The resolution width increases linearly as targets shift outside of the orbit in the radial dimension. The Doppler bandwidth decreases as the targets approach the center of the orbit. This implies that for targets located on the orbit plane and bounded by the orbit, the required PRF is proportional to the distance from target to orbit center.

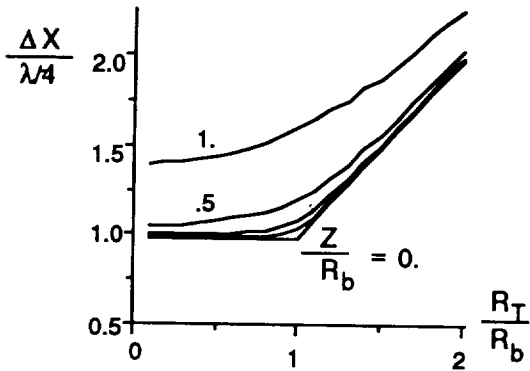


Figure 4.a Resolution vs target location

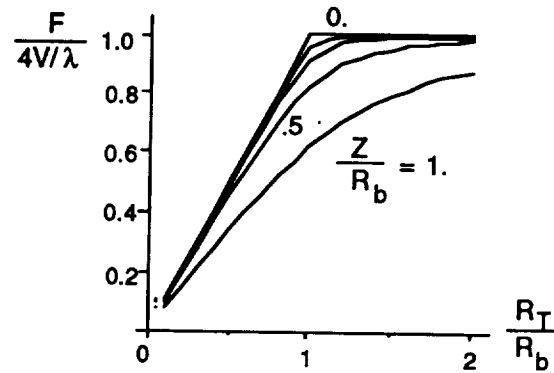


Figure 4.b Bandwidth vs target location

Consider a special case where $Z=0$ and R_T approaches R_b . According to the bandwidth equation given above, we may find that the required PRF is equal to $4v/\lambda$. This indicates that the required sampling spacing is exactly $\lambda/4$ which equals to the ultimate azimuth resolution. The time interval of the principle aperture is given by

$$T_p(Z, R_T) = \frac{2R_b}{v} \cos^{-1} \left(\frac{-A + (A^2 - B^2)^{1/2}}{B} \right)$$

It will be more convenient to express the aperture time interval as a value normalized by the period of a complete flight circle. The complexity of SAR processing is usually determined by the number of samples within the aperture or the value of the time-bandwidth product TBP given by $TBP(Z, R_T) = T(Z, R_T)F(Z, R_T)$. The time interval and time-bandwidth product of the principle aperture are shown in Figure 5.a and 5.b.

In summary, the analysis in this section leads to the determination of the PRF for operating the spotlight radar, the predicted resolution, the time interval of the aperture and the time-bandwidth product to be selected for signal processing.

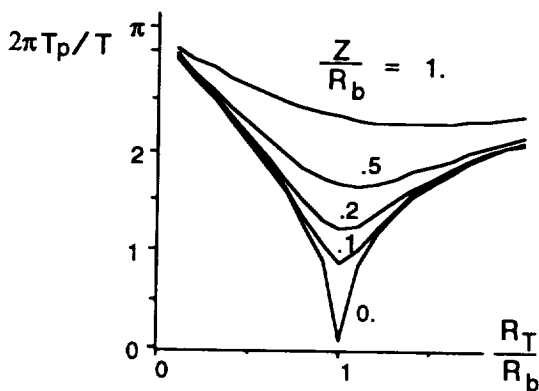


Figure 5.a Aperture Interval vs target location

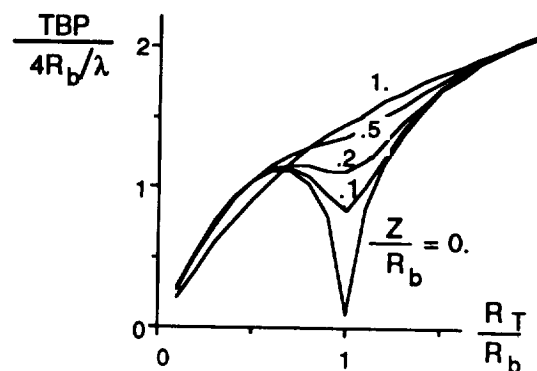


Figure 5.b Time-bandwidth product vs target location

PROCESSING ALGORITHM

Several algorithms were presented for processing spotlight-mode SAR data or the rotating object data. These algorithms include the well known range-Doppler algorithm applied to sub apertures, the backprojection processing method (Munson, et. al., [2]) commonly used in computer-aided tomography (CAT), and the polar format processing algorithm (Ausherman, et. al [3]). One essential assumption required for both the CAT and polar algorithms is that the dimension of the imaged area is much less than the radar to target distance. Other processing algorithms devised for imaging rotating object include a tomographic extension of Doppler processing algorithm (Mensa, et. al. [4]) and a range-Doppler processing algorithm (Walker, J. [5]). The first method is suitable only for imaging sparse arrays of objects due to its higher integrated sidelobe ratio (ISLR); and both algorithms also rely on the assumption of large radar to target distance. An exact solution for a circular aperture acoustic imaging system was presented by Norton [1]. This algorithm requires the implementation of a quasi fast Hankle transform which is not very efficient.

The difficulty in processing spotlight-mode SAR data collected from a circular path is that the Doppler history of a point target involves many higher order terms and that the depth of focus is very shallow. To overcome the first problem, the algorithm proposed here make use of an exact 2-D spectrum of a point target (Jin, 1992 [6]) in a range Doppler like processing approach. To overcome the second problem, this algorithm updates its reference function as frequently as required.

According to [6], the magnitude and the phase of a reference spectrum are given by

$$A(\omega_r, \omega) = \sqrt{2\pi} \left| \frac{d^2(-(\omega_r + \omega_0) \cdot 2R(t_s) / c)}{dt^2} \right|^{-1/2}$$

$$\psi(\omega_r, \omega) = \exp \left\{ j \left(\frac{\cos^{-1}(\alpha(\omega_r, \omega)) \omega}{v / R_b} - 2k_r \sqrt{A + B\alpha(\omega_r, \omega)} - \frac{\pi}{4} \right) \right\}$$

where ω is the azimuth angular frequency, ω_r is the range angular frequency, ω_0 is the angular frequency of the carrier, K_r is equal to ω_r/c , where c is the speed of light, and

$$\alpha(\omega_r, \omega) = \left(-\frac{\omega^2}{k_r^2} \pm \sqrt{\frac{\omega^4}{k_r^4} + 4 \frac{\omega^2 v^2}{k_r^2 R_b^2} (B - R_0^2) + 4 \frac{\omega^4}{k_r^4} B^2} \right) / 2 \frac{v^2}{R_b^2} B$$

The energy distribution of the 2-D spectrum of a point target is given in Figure 6. It can be seen that the amount of area with energy is proportional to the distance from the target to the center point.

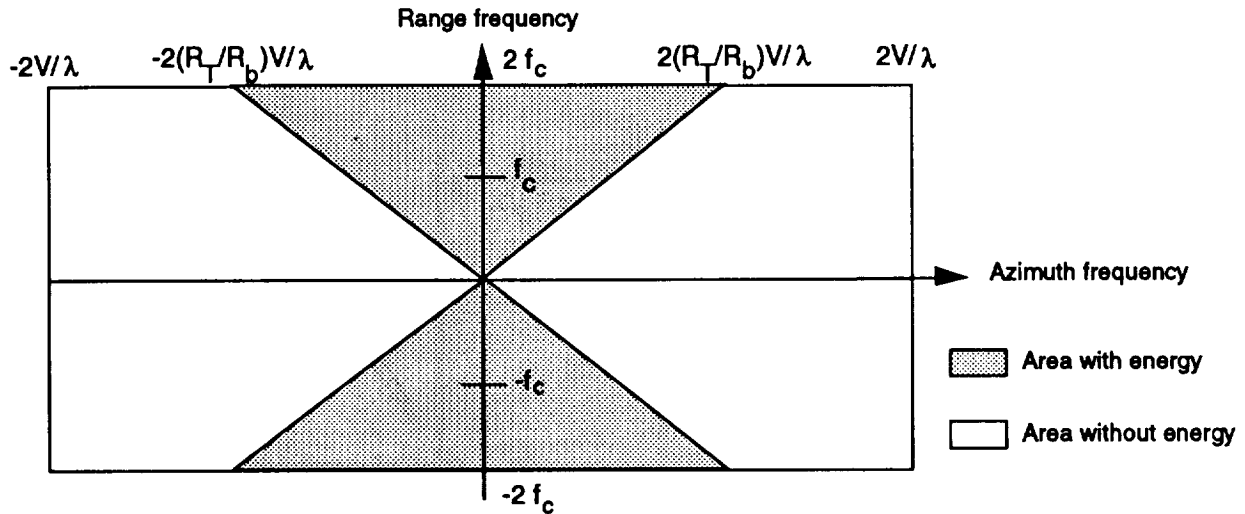


Figure 6. The 2-D spectrum of a point target

The basic correlation steps for the spotlight-mode processing are summarized below.

- (1) Perform subsampling for the echo pulses according to the radius of the spot area. This step is not required if the PRF of the sensor is tuned to that radius such that there is no redundant data. Transform the SAR data into its spectrum by a 2-D FFT process.
- (2) Perform a 2-D SAR correlation. For each azimuth line with a constant range position, a reference spectrum is generated according to equation (1). Correlation is performed by multiplying the data spectrum and the conjugated reference, averaging in range, and performing an inverse azimuth FFT. This is repeated for each azimuth line.
- (3) Perform geometric resampling to correct for the geometry and grid spacing. The mapping between image pixels generated from step (2) and points on the ground for a spotlight-mode SAR is given in Figure 7.

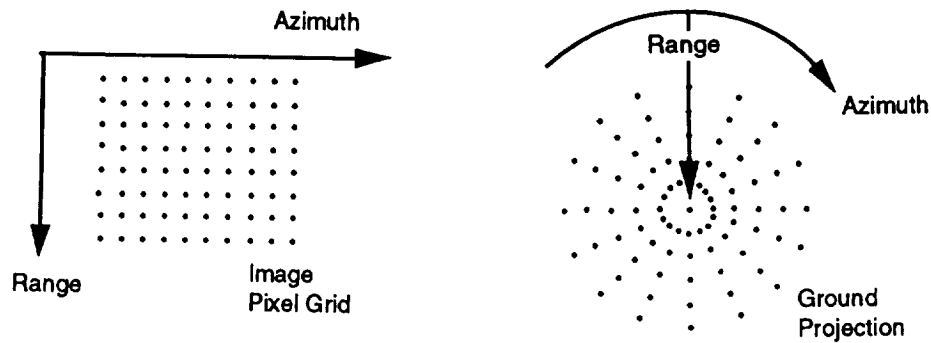


Figure 7. Image pixel to projection mapping in a spotlight mode SAR

COMPUTATION EFFICIENCY

The algorithm described above takes the advantage of computation efficiency of FFT operations. Therefore, it is a highly efficient algorithm as compared to a previous algorithm proposed by Norton [1]. To illustrate this, the Norton's algorithm is briefly reviewed first.

Let $f(r, \theta)$ denotes the reflectivity of the medium and $g(r, \theta)$ denotes the echo signals received in a polar coordinate with radial position r and angle θ . $f(r, \theta)$ can be recovered by the following three steps:

- (1) Perform spherical harmonic expansion for $g(r, \theta)$ for its coefficients,
$$g_n(r) = \frac{1}{2\pi} \int_0^{2\pi} g(r, \theta) e^{-in\theta} d\theta$$
- (2) Get the spherical harmonic expansion coefficients $f_n(r)$ of $f(r, \theta)$ by
$$f_n(r) = H_n \left\{ \frac{1}{J_n(Rz)} H_0 \left\{ \frac{g_n(\rho)}{2\pi\rho} \right\}_z \right\}_r$$
- (3) Reconstruct $f(r, \theta)$ from $f_n(r)$ by
$$f(r, \theta) = \sum_{n=-\infty}^{\infty} f_n(r) e^{in\theta}.$$

In the second step, Hankle's transform of the 0-th order and n-th order are implemented by a quasi fast Hankle transform. It is assumed that in both algorithms the reference functions are generated before processing and permanently stored in the computer memory. The computation efficiency will be examined only on the amount of complex multiplies performed to yield an image of a diameter of $2N$ pixels. These results are summarized in Table I and Table II.

Table I. Amount of complex multiply in spotlight mode algorithm

| PROCESSING STEP | 2-D FFT FOR ECHO DATA | REFERENCE MULTIPLY | 1-D INVERSE FFT |
|--------------------|---|--------------------|------------------------------|
| NUMBER OF MULTIPLY | $\pi N^2 \text{Log}_2 \pi N$ $+\pi N^2 \text{Log}_2 N$ | $\pi N^3 / 2$ | $\pi N^2 \text{Log}_2 \pi N$ |

Table II. Amount of complex multiply in Norton's algorithm

| PROCESSING STEP | HARMONIC EXPANSIONS | REFERENCE MULTIPLY | 1-D HANKLE TRANSFORMS |
|--------------------|-------------------------------|---|---|
| NUMBER OF MULTIPLY | $2\pi N^2 \text{Log}_2 \pi N$ | $\pi N N_h$ $N_h = K_1 N \text{Ln}(K_2 N)$ | $2N_h \text{Log}_2 N_h$, $N_h = K_1 N \text{Ln}(K_2 N)$ |

The disadvantage of the quasi fast Hankle transform is that data samples must be oversampled from N to $N_h = K_1 N \text{Ln}(K_2 N)$, where K_1 and K_2 are constants. This oversampling increase the amount of data and the amount of multiplies. The computation bottleneck of the spotlight algorithm is in the reference multiply which is proportional to N^3 . For N being 128 to 512 points, the amount of multiplies in the spotlight algorithm is from 1/10 to 1/4 times of that in Norton's algorithm. Since a large portion of the point target spectrum has no energy as shown in Figure 6, the amount of multiply can further be reduced by a factor of two in reference multiply and inverse FFT processes.

SIMULATION

A simulation was performed to test the proposed algorithm and to verify the analysis on the azimuth resolution. Plotted in Figure 7.a and 7.b. are the impulse responses of two aircraft spotlight systems, both with zero altitude. The first one has a range bandwidth being twice the carrier frequency such that the range resolution is comparable to the azimuth resolution. The second system has a range bandwidth of .15 times the carrier frequency. The 3-dB resolutions in range and azimuth of the first system are very close to $\lambda/4$. The 3-dB resolutions of the second system are also close to $\lambda/4$. However, it has a much worse integrated sidelobe ratio.

Range Bandwidth = 2 x Radar Carrier Frequency

Range Bandwidth = 0.15 x Radar Carrier Frequency

Full Resolution Processing over the Principle Aperture

Full Resolution Processing over the Principle Aperture

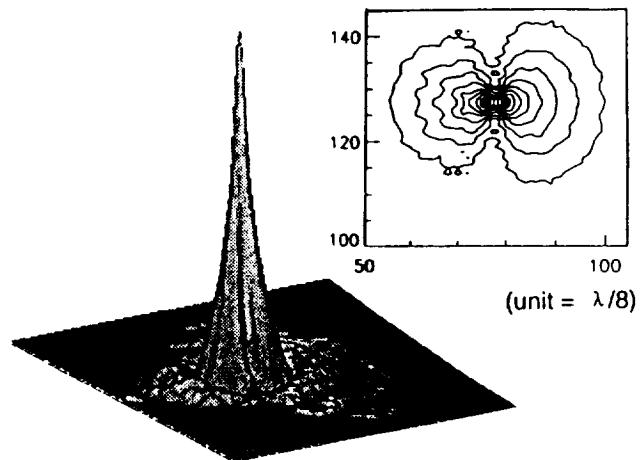
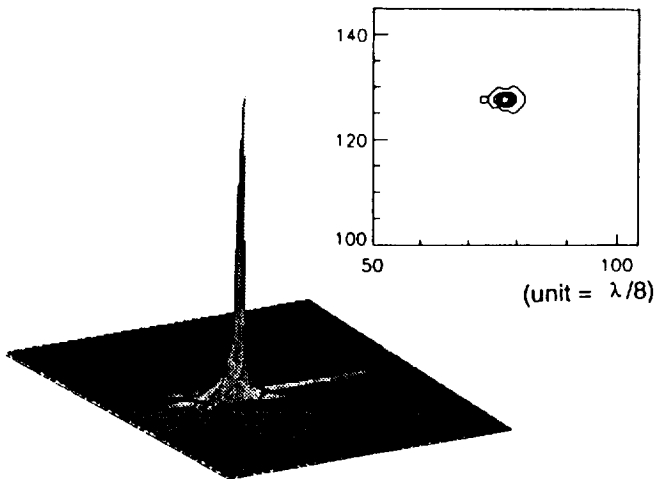


Figure 7.a Spotlight SAR impulse response

Figure 7.b Spotlight SAR impulse response

CONCLUSION

The spotlight-mode aircraft SAR in a circular flight path has been analyzed in terms of resolution, bandwidth, aperture arc, and the time-bandwidth product. An exact and efficient processing algorithm is proposed to recover spotlight-mode SAR images. The simulation result of the point-target response indicates that for full azimuth resolution processing both the azimuth and range 3-dB resolution can achieve the ultimate resolution of $\lambda/4$, regardless of the range bandwidth. This algorithm is directly applicable to ultrasonic reflectivity tomography system. With further optimization in computation efficiency, the processing throughput rate shall be about ten times faster than a previously proposed algorithm.

ACKNOWLEDGMENTS

The research described in this paper was carried out by the Jet Propulsion Laboratory, California Institute of Technology, under a Contract with the National Aeronautics and Space Administration.

Reference:

- [1] Norton, Stephen J., "Reconstruction of a Two-Dimensional Reflecting Medium over a Circular Domain: Exact Solution", *J. Acoust. Soc. Am.*, 67(4), 1980.
- [2] Munson, D. C., O'Brien J. D., and Jenkins, W. K., "A Tomographic Formulation of Spotlight-Mode Synthetic Aperture Radar", *Proceedings of the IEEE*, Vol. 71, No. 8, August, 1983.
- [3] Ausherman, Dale A., et. al., "Developments in Radar Imaging", *IEEE Trans. on Aerospace and Electronic Systems*, Vol. AES-20, No. 4, July, 1984.
- [4] Mensa, D., Heidbreder, G., and Wade, G., "Aperture Synthesis by Object Rotation in Coherent Imaging", *IEEE Trans. on Nuclear Science*, Vol. NS-27, No. 2, April 1980.
- [5] Walker, Jack L., "Range-Doppler Imaging of Rotating Objects", *IEEE Trans. on Aerospace and Electronic Systems*, Vol. AES-16, No. 1, January, 1980.
- [6] Jin, Michael Y., "An Exact Processing Algorithm for Wide Beam Spaceborne SAR Data", *ISY Conference, ERS-1/JERS-1 Workshop*, Tokyo, November, 1992.